Phospholipase A_2 Hydrolysis of Supported Phospholipid Bilayers: A Neutron Reflectivity and Ellipsometry Study[†]

Hanna P. Vacklin,*[,‡] Fredrik Tiberg,[§] Giovanna Fragneto,[||] and R. K. Thomas[‡]

Oxford University, Physical and Theoretical Chemistry Laboratory, South Parks Road, Oxford OX1 3QZ, United Kingdom, Camurus AB Ltd., Ideon Science Park, Gamma 2, SE-223 70 Lund, Sweden, and Institut Laue-Langevin, 6 rue Jules Horowitz, BP 156, 38042 Grenoble, France

Received October 25, 2004; Revised Manuscript Received December 9, 2004

ABSTRACT: We have investigated the phospholipase A_2 catalyzed hydrolysis of supported phospholipid bilayers using neutron reflection and ellipsometry. At the hydrophilic silica−water interface, hydrolysis of phosphatidylcholine bilayers by phospholipase A_2 from *Naja mossambica mossambica* venom is accompanied by destruction of the bilayer at an initial rate, which is comparable for DOPC and DPPC but is doubled for POPC. The extent of bilayer destruction at 25 °C decreases from DOPC to POPC and is dramatically reduced for DPPC. Neutron reflectivity measurements indicate that the enzyme penetrates into the bilayers in increasing order for DOPC, POPC, and DPPC, while the amount of enzyme adsorbed at the interface is smallest for DPPC and exhibits a maximum for POPC. Penetration into the hydrophobic chain region in the bilayer is further supported by the fact that the enzyme adsorbs strongly and irreversibly to a hydrophobic monolayer of octadecyltrichlorosilane. These results are rationalized in terms of the properties of the reaction products and the effect of their accumulation in the membrane on the kinetics of enzyme catalysis.

Phospholipase A_2 catalyses the hydrolysis of *sn*-1,2-diacyl-phospholipids into an *sn*-1-acyl-lyso-phospholipid and a fatty acid, and it belongs to a class of soluble enzymes that function at the polar−apolar interface between a membrane and water (*1, 2*). PLA_2[1] enzymes occur in a wide range of environments and perform an amazing variety of biological functions, but their overall structure and catalytic site mechanism are conserved across species and class (*2, 3*). The ternary structure of *Naja naja naja* PLA_2, which is common to all Indian cobra venoms, is shown in Figure 4a. Apart from many invertebrate and insect venoms, PLA_2's are found both inside and outside cells, where they play a key role in phospholipid remodeling (*4, 5*), signal transduction (*6, 7*), and production of arachidonic acid (*8*−*11*), a precursor to the inflammatory mediators prostaglandins and eicosanoids (*12*). Considering the evidence that PLA_2's participate in host defense at both local and systemic levels (*13*), they are a potential target for drug development aimed at their inhibition (*14*) and drug delivery based on their selective activation at the site of inflammation (*15*).

The PLA_2's are water soluble but only act when they adsorb at a membrane surface. They are therefore heterogeneous catalysts, which means that conventional kinetic measurements cannot discriminate the different rate processes when there is an equilibrium between surface and bulk. The heterogeneity of the reaction also diminishes the usefulness of the atomic resolution structures of the PLA_2's (*16*−*19*), because PLA_2 interaction with the membrane is an interaction with an *assembly* of molecules (*20*), whose collective response may be more important than the specific catalytic site mechanism in determining the course of hydrolysis.

To date, research on PLA_2 kinetics has largely been carried out in bulk phospholipid dispersions or in Langmuir monolayers at the air−water interface. In vesicle or micelle dispersions, only the overall rate of product formation can be monitored (*21*−*23*), and no information has been obtained about the location of the enzyme or the distribution of reaction products between the surface and bulk phases. At the air−water interface, kinetic experiments have been limited to short-chain phospholipids, which have soluble reaction products and allow the membrane composition to be maintained constant (*24*). In a typical biological membrane, however, the products are usually of limited solubility, and their accumulation in the membrane can change its physical properties and morphology significantly. In either case, the research has been largely limited to saturated chain phosphatidylcholines, although oleic acid and other 9-cis unsaturated fatty acids are very common in natural membranes, and the presence of such double bonds is known to have a great effect on both molecular and membrane properties (solubility, compressibility, and morphology). For example, fluorescence microscopy studies of asymmetric

[†] This work was supported by the UK Biotechnology and Biological Sciences Research Council (BBSRC), the EU Marie Curie training network, the Academy of Finland, and the Finnish Cultural Foundation.

* Corresponding author. E-mail address: hanna.vacklin@chem.ox.ac.uk. Telephone: +44186527455. Fax: +441865275410.

[‡] Oxford University.

[§] Camurus AB Ltd..

[||] Institut Laue-Langevin.

[1] Abbreviations: DOPC, L-α-1,2-*O*-dioleyl-3-*O*-*sn*-glycerophosphocholine; DPPC, L-α-1,2-*O*-palmitoyl-3-*O*-*sn*-glycerophosphocholine; POPC, L-α-1-*O*-palmitoyl-2-*O*-oleyl-3-*O*-*sn*-glycerophosphocholine; PLA_2, phospholipase A_2; DDM, *n*-β-D-docecyl maltoside; *d*-OTS, perdeuterated octadecyl trichlorosilane; CmSi, water contrast matched to bulk silicon. A list of symbols is given.

10.1021/bi047727a CCC: $30.25 © xxxx American Chemical Society
Published on Web 00/00/0000 PAGE EST: 10.1

phospholipid monolayers have revealed that the morphological changes induced by PLA_2 hydrolysis are very sensitive to the solubility of the fatty acid product in particular (*25, 26*). Brewster angle microscopy (*27, 28*), atomic force microscopy (*29, 30*) and cryo-transmission electron microscopy (*31*) have been used to detect membrane break up in supported bilayers as well as monolayers and liposomes, but these methods lack the resolution to detect the presence of the enzyme directly. To understand how the physical interactions between PLA_2 and a membrane interface regulate enzymatic hydrolysis, it is desirable to monitor the membrane association of the enzyme together with the structural and compositional changes induced by the hydrolytic reaction.

In this paper we describe the application of specular neutron reflection and ellipsometry to monitor the hydrolysis of supported phosphatidylcholine bilayers by phospholipase A_2 from *Naja mossambica mossambica* venom. We have recently developed a method for depositing phospholipid bilayers on silicon supports by coadsorption with a soluble surfactant (*32*), and we have shown that surfactant-free bilayers can be formed from phospholipids with varying degrees of unsaturation (*33, 34*). An advantage of using self-assembled supported bilayers as a substrate is that their structure and composition can be determined in-situ by neutron reflection prior to the introduction of the enzyme.

Specular neutron reflection and ellipsometry are techniques that noninvasively probe interfacial structures. In both cases, the structural parameters (thickness, surface coverage, refractive index) of an adsorbed film are derived from variation in reflected intensity as a function of angle (neutrons) or polarization (ellipsometry). Ellipsometry has a time-resolution that enables the observation of adsorption/desorption kinetics, while neutron reflection offers the unique power of contrast variation. Essentially, the neutron refractive index of hydrogenous materials can be manipulated by deuterium exchange, making it possible to obtain several independent reflectivity profiles from the same *chemical* situation. Both methods are suitable for structure determination in systems that exhibit no lateral ordering in the interfacial plane, as is typical of biological membranes, and can be employed at buried interfaces (i.e. under water).

1. NEUTRON REFLECTION

Neutron reflection measures the structure and composition of an adsorbed thin layer perpendicular to the interface, and experiments are routinely performed at both air−liquid and liquid−solid interfaces. The sensitivity of neutron reflectivity to the layer structure depends on its scattering contrast to the surrounding media. The reflection of neutrons gives rise to interference fringes from a thin film, whose thickness is related to the fringe separation and whose reflection amplitude is proportional to the scattering length density profile of the system. The neutron scattering length density $\rho(z)$ is defined in eq 1,

$$\rho(z) = \sum_j n_j(z) b_j \tag{1}$$

where b_j is the neutron scattering length of nucleus j and $n_j(z)$ is the number density of nuclei in the direction of the surface normal. For a planar adsorbed film, the specular reflectivity $R(\rho)$ can be calculated using an optical matrix model (*35*), which divides the surface region into homogeneous layers distinguished by their scattering length density. The calculated reflectivity is fitted to experimental results using a computer program such as the AFit (v. 3.1) program (*36*), which uses the optical matrix method and allows the simulation of reflectivity profiles by characterizing each layer by its thickness, scattering length density, solvent volume fraction, and roughness.

In the case of a mixed layer of two or more components, the resultant scattering length density will be a sum of the individual scattering length densities of all the components weighted by the volume fractions at which they are present in the layer. For example, in a mixture of phospholipid (l), enzyme (E), and water (w), the scattering length density will be

$$\rho_{\text{layer}} = \phi_{\text{l}}\rho_{\text{l}} + \phi_{\text{E}}\rho_{\text{E}} + \phi_{\text{w}}\rho_{\text{w}} \tag{2}$$

The thickness resolution of neutron reflection can be of the order of 1 Å at high contrast, and in particular, it can be increased by use of contrast variation (*37*), that is, altering the scattering length density profile via deuteration of the solvent and/or film. The accuracy of the model structure is improved by simultaneous fitting of reflectivity profiles of the same system in different contrasts, that is, constraining the isotopically different situations to the same physical structure. This way, for a phospholipid bilayer supported at the silica−water interface, the overall bilayer thickness and hydration should be the same for a hydrogenated phospholipid in D_2O ($\rho = 6.35 \times 10^{-6}$ Å^{-1}) and a deuterated phospholipid in water contrast matched to silicon ($\rho = 2.07 \times 10^{-6}$ Å^{-1}). The silica−D_2O contrast is very sensitive to the volume fraction of hydrogenous phospholipids and also other molecules with low scattering length densities.

To construct a bilayer model for fitting, we used phospholipid volume fractions from molecular dynamics simulations of DOPC, POPC, and DPPC bilayers (*38*), that have been shown to agree excellently with experimental data (*39−42*). For phospholipase A_2, the scattering length was calculated from the *Naja mossambica mossambica* amino acid sequence (*43, 44*) and the molecular volume was estimated from amino acid volume data adapted for aqueous solutions (*45*). The scattering length density of PLA_2 was calculated by taking into account the number of exchangeable protons in each polar amino acid residue (*46*).

The component volumes and scattering length densities used in data fitting and calculations are shown in Table 1. In the AFit program, the reflectivity profile of the pure phospholipid bilayer was first fitted using a three-layer model, assuming that the headgroups and hydrocarbon chains could be modeled as noninterpenetrating homogeneous slabs. The thickness and solvent content of the hydrocarbon core (which are the most sensitive parameters of the bilayer in D_2O) were fitted to the observed reflectivity, and the solvent fraction in the headgroup region was adjusted using a stoichiometric constraint, that is, that the area per molecule must remain constant to within ±1 Å^2 throughout the bilayer. This constraint requires that the number of headgroups and chains in the bilayer must agree to within 2%, and it was the minimum practicable value with which good quality fits could be found to all the data sets. The area per molecule itself was not one of the fitting variables and has an error

Table 1: Scattering Length Densities and Molecular Properties of Phospholipids and Phospholipase A_2[a]

	h-DPPC	DOPC	POPC	*Naja m. mossambica* PLA_2
b ($\times 10^{-5}$ Å^{-1})	27.5	39.1	33.3	558
V_{mol} (Å^3)	1215.8	1322.8	1255.9	15451
M (g mol^{-1})	734.0	786.0	760.0	13219
ρ ($\times 10^{-6}$ Å^{-2})	0.226	0.296	0.265	3.61
$V_{headgroup}$ (Å^3)	326.3	337.1	322.1	
$\rho_{headgroup}$ ($\times 10^{-6}$ Å^{-2})	1.84	1.78	1.86	
V_{chains} (Å^3)	889.2	985.0	933.7	
ρ_{chains} ($\times 10^{-6}$ Å^{-2})	−0.37	−0.21	−0.29	

[a] Molecular volumes are calculated from phospholipid component volumes obtained from bilayer molecular dynamics simulations (*38*), and from amino acid volume data adapted for aqueous solutions (*45*).

associated with it, which is derived directly form the acceptable variation in the bilayer thickness and lipid volume fraction and listed in the tables of results. It was not necessary to incorporate any interfacial roughness into the bilayer model, nor was a solvent layer of the dimensions previously suggested (*47, 48*) found to be present between the headgroups and the SiO_2 surface. We believe that it is possible that the absence of the solvent layer may be related to the method used in the formation of supported bilayers, which in our case was from lipid−surfactant micelles as opposed to Langmuir−Blodgett or vesicle deposition. If quartz is used as a substrate, the surface can develop a thick (up to 200 Å) gel layer with a large fraction of water (65%), which can be misinterpreted as a layer of solvent in data fitting (*49*).

2. ELLIPSOMETRY

We used multiple-medium null ellipsometry (*50*) to follow the hydrolysis of phospholipid bilayers, that had been previously formed in-situ. The ellipsometric angles ψ and Δ were determined from measurement of the incident and final angles of polarization and are used to compute the complex reflection amplitude ratio ρ:

$$\rho = |\frac{r_p}{r_s}| \exp(\delta_{rp} - \delta_{rs}) = \tan \psi \exp(i\Delta) \qquad (3)$$

where r_s and r_p are the reflection coefficients for s- and p-polarizations and δ_{rs} and δ_{rp} represent their phase shifts upon reflection. An optical model for the solid substrate was first derived by measuring its ellipsometric angles in air and water (*50*). This was done to find the oxide layer thickness in order to accurately characterize the thickness of the phospholipid bilayers. We used a three-layer model to characterize the silicon−silicon oxide air/water system to yield values for the silicon refractive index of $n_2 = (5.5 \pm 0.05) - (0.25 \pm 0.05)j$ and $n_1 = 1.48 \pm 0.005$ for the oxide layer, whose thickness was typically 270−300 Å. All measurements were done at a wavelength of 4015 Å and an incident angle of ∼68°.

During phospholipid adsorption and phospholipase hydrolysis the ellipsometric angles were recorded every 3−60 s, and using a four-layer model based on the previously determined substrate model, the bilayer surface excess was computed using de Feijter's method of finding the surface excess of a surfactant as in eq 4.

$$\Gamma = \frac{(n - n_0)}{dn/dc} d \qquad (4)$$

n and n_0 are the refractive indices of the adsorbate and bulk solvent, respectively, d is the adsorbed film thickness, and dn/dc is the refractive index increment of the adsorbate measure by classical refractometry. For all phospholipids we used a dn/dc value of 0.154, which has been measured for DOPC. The standard deviation in determining the ellipsometric angles ψ and Δ was estimated previously to be of the order of 0.001° and 0.002°, respectively (*50*). Although the errors in thickness and refractive index can be quite large at low adsorbed amounts, they fall to <5% above 2 mg m^{-2} and are coupled in a way which cancels out when the surface excess is computed. Thus, the surface excess is the most reliably computed property of very thin films (<30 Å) and was our primary interest in these experiments.

3. EXPERIMENTAL SECTION

Ultrahigh quality water ($\Omega = 18.2\ \Omega$) was used in all experiments. D_2O for experiments was provided from the reactor at the Institut Laue Langevin, Grenoble. The phospholipids, phospholipase from *Naja mossambica nossambica* (P7778, 1500 units/mg), Tris-buffer, and β-D-dodecyl maltoside were purchased from Sigma-Aldrich at 99% purity and used without further purification. The solid supports for neutron reflection were polished in house and cleaned for 15 min in a mixture of 1:4:5 $H_2O_2/H_2SO_4/H_2O$ at 80−85 °C, followed by ozonolysis on the day of the experiment (*51*). This treatment leaves a natural oxide layer of 7−10 Å thickness and 3−5 Å roughness with 5−10% water on the Si(111) surface. For ellipsometry, p-type boron doped (100) silicon wafers were preoxidized to 300 Å by baking for 1 h at 920 °C. The wafers were cleaned by (i) 1:1:5 $H_2O_2/NH_3/H_2O$ for 10 min and (ii) 1:1:5 $H_2O_2/HCl/H_2O$ before ultrasonication in water (18.2 Ω) and ethanol. The slides were stored in ethanol until use and dried and plasma-cleaned at 3×10^{-2} mbar for 5 min in a Harris Scientific PDC-3XG plasma cleaner.

Neutron reflection experiments were carried out on the D17 reflectometer at the Institute Laue-Langevin in Grenoble, France. All measurements were done in the time-of-flight mode, using wavelengths of 2.2−19 Å on D17. The sample solution is contained in a Teflon trough clamped against the Si surface with hollow aluminum plates that allow temperature equilibration by a circulating water bath to an accuracy of ±0.3 °C. The cell has an inlet and outlet, allowing the change of contents without exposing the surface to air, and a cavity for a magnetic flea for stirring the bulk solution.

A typical neutron experiment procedure for has three separate stages: characterization of the silica support, adsorption of the phospholipid bilayer from a 6:1 w/w mixture of β-D-dodecyl maltoside and the requisite phospholipid, and injection of 0.2 mg/mL phospholipase in buffer solution (10 mM Tris-HCl at pH 7.4). All manipulations were performed in-situ in the neutron reflectometer, with reflectivity recorded before and after phospholipid adsorption and continuously during PLA_2 hydrolysis. In an ellipsometry experiment, the substrate SiO_2 layer is first characterized in water and in air, and the ellipsometric angles are recorded continuously during bilayer formation and enzyme hydrolysis.

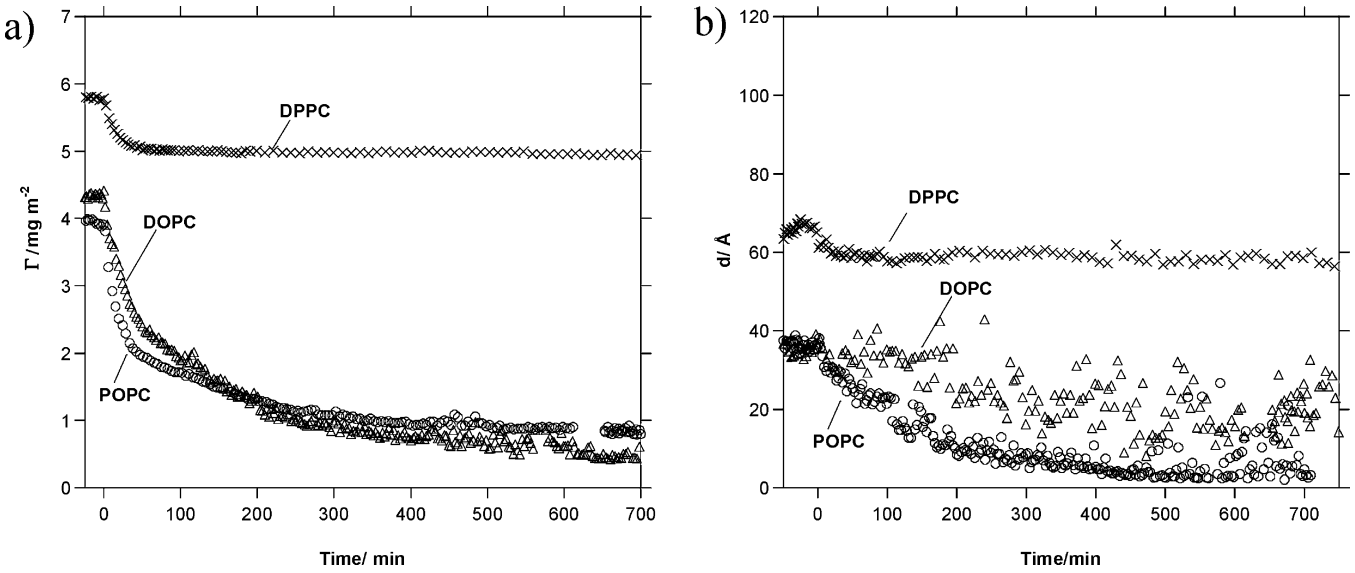

FIGURE 1: Changes in (a) surface excess and (b) bilayer thickness during hydrolysis of DOPC, POPC, and DPPC supported bilayers.

Ellipsometry experiments were carried out using a Rudolph Research thin film ellipsometer type 43603-200E, which has a vertical reflection geometry. The angle of incidence for all measurements was ~68 ± 0.5°, for which a trapezoidal quartz cuvette was used to provide normal incidence to the beam. The sample cell was kept at 25 ± 0.3 °C by a circulating water bath, and further details of the experimental set up have already been published elsewhere (*52*). The substrate was characterized in air and water, and optical imperfections of the instrument were accounted for by performing four-zone averaging (*53*) of the substrate ellipsometric (nulling) angles. Both phospholipids and phospholipase were introduced by dilution of a small aliquot (10−250 μL) into the cuvette volume (5 mL).

Phospholipid bilayers were formed by adsorption of micellar mixtures of the phospholipids with the sugar-surfactant *n*-β-D-dodecyl maltoside, the details of which have been published elsewhere (*33, 34*). Gradual dilution of the bulk micellar solution leads to preferential adsorption of the phospholipid while all surfactant is removed by rinsing, leaving behind a well-characterized supported bilayer.

4. RESULTS

4.1. Ellipsometry. The hydrolysis of DOPC, POPC, and DPPC bilayers by PLA_2 from *Naja mossambica mossambica* venom was investigated using ellipsometry and neutron reflection. Figure 1 shows the evolution of bilayer thickness d and surface excess Γ as a function of time for the three lipids after the introduction of 0.02 mg/mL PLA_2 at $t = 0$. In all cases, hydrolysis causes a gradual removal of the bilayer from the silicon−water interface, but the rate and extent of reaction are different in each case. After 14 h the reaction has become very slow for DOPC and POPC, and at this point their surface excess values are 0.5 and 0.75 mg m^{-2}, respectively (Table 2). These correspond to 11% and 19% of the original bilayer mass, which was somewhat higher for DOPC than POPC. The initial rates of decrease in surface excess were analyzed using a linear curve fit and found to be 0.803 μmol m^{-2} s^{-1} (DOPC), 2 μmol m^{-2} s^{-1}(POPC), and 0.8 μmol m^{-2} s^{-1} (DPPC). In the case of DPPC, however, although the initial rate is comparable to DOPC, the reaction stops after only 14% or 0.8 mg m^{-2} has been removed.

Table 2: Summary of Ellipsometry Results on Bilayer Hydrolysis by 0.02 g/L *Naja mossambica mossambica* Phospholipase A_2[a]

	DOPC	POPC	DPPC
bilayer surface excess (mg m^{-2}/μmol m^{-2})	4.4/5.6	4.0/5.2	5.8/7.9
initial slope (μmol m^{-2} s^{-1})	0.8	2.0	0.8
final surface excess (mg/μmol m^{-2})	0.50/0.6 (11%)	0.75/1.0 (19%)	5.0/ 6.8 (86%)

[a] The figures in parentheses indicate the amount of bilayers removed relative to its original mass.

The behavior of POPC during hydrolysis is qualitatively similar to that of DOPC, but the rate of disappearance of material is initially faster for POPC, which seems counterintuitive because it is the more saturated of the two. One would expect the partitioning of lyso-palmitoyl-phosphocholine into the solution phase to be a slower process than that of unsaturated lyso-oleyl-phosphocholine, as, in terms of the solubility of a hydrocarbon chain, a double bond is generally equivalent to reducing the number of carbons by two. DPPC, on the other hand, shows remarkably different behavior, even though the PLA_2 catalytic rate as such is not thought to be sensitive to the hydrocarbon chains of the substrate. The differences in the cases of POPC and DPPC are the initial state of the bilayer, and the nature of the fatty acid produced. As POPC is hydrolyzed, oleic acid and lyso-palmitoyl-PC are created, whereas the initially condensed DPPC bilayer becomes a mixture of DPPC, palmitic acid, and lyso-palmitoyl-PC.

Differential scanning calorimetry and FTIR studies on the effect of fatty acids in PC bilayers (*54*) have shown that the presence of palmitic acid causes a significant increase in the rigidity of a DPPC bilayer but that the presence of oleic acid causes only a small lowering of the main phase transition and no change in the packing of DPPC. At the same time, neither lyso-PC nor fatty acid leads to significant permeability in fluid bilayers, even though their effects on condensed bilayers are dramatic (*55*).

The effect of fatty acids and lysolipids on bilayer properties can be used qualitatively to explain the difference in the

behavior of bilayers during hydrolysis. In DOPC and DPPC bilayers the initial rate of removal from the interface is virtually identical, and this suggests that the enzyme initially interacts with both bilayers in a similar way. The condensed nature of the DPPC bilayer can however cause a reduction in enzyme penetration into the layer or a significant decrease in the diffusion rate of the enzyme at the interface. The accumulation of palmitic acid in the DPPC bilayer leads to an even tighter packing of the lipid material but also an increased electrostatic attraction to the enzyme due to the negative charge. The reaction would then grind to a halt when the enzyme either is pushed out of the membrane entirely or is bound too tightly in fatty-acid-rich regions to access the substrate molecules by diffusion. Our observations of the rates of desorption are consistent with fluorescence microscopy results on 6,16-PC and 16,6-PC monolayers (*25*), where PLA_2 action caused phase separation in the palmitic acid containing membranes, but not if the fatty acid product was the soluble caproic acid, with the PLA_2 itself accumulating at the domain edges of the condensed regions.

The POPC bilayer should have a lower mean density initially than DOPC due its slightly lower surface excess, and neither the lyso-palmitoyl-PC nor the oleic acid product should have a significant effect on the packing or permeability of the membrane. A lower membrane density should create more room for the enzyme to access the membrane and/or to diffuse more freely, and this could explain the initially higher rate of disappearance of material from the interface. At the enzyme concentration used (0.02 mg/mL), not all the enzyme is initially bound to the membrane and there is also a replenishing pool of enzyme in the bulk solution that can be attracted to the bilayer as negative charge accumulates.

What causes the desorption of material as a result of hydrolysis cannot be determined without the knowledge of the distribution of the products and phospholipid between the surface and the bulk phases as the reaction proceeds. We have in this instance used neutron reflection to elucidate the differences between phospholipids by determining the amount and location of the enzyme at the interface.

4.2. Neutron Reflectivity. Phospholipid bilayers were formed by coadsorption of lipid with β-D-dodecyl maltoside on SiO_2 surfaces previously characterized in D_2O. After recording the reflectivity of each bilayer, a small amount of enzyme stock solution (3−5 mL) was injected into the sample cell (15 mL), and changes in reflectivity were typically monitored overnight. In each case, advantage was taken of the ability of time-of-flight reflectometry (*56*) to capture 10−20 min "snapshots" of the initial changes in reflectivity. Because specular reflectivity decreases rapidly with increasing angle of incidence, this was done at a low enough angle (in this case 0.8°) to allow reliable data collection in 10 min. The q-range obtainable at any given angle depends on the available range of neutron wavelengths, and in this case $\lambda = 2-20$ Å enabled us to record reflectivity from the critical edge ($q = 0.0148$ for the interface between Si and D_2O) up to $q \sim 0.1$ Å^{-1}. The presence of a region of total reflectivity (i.e. $R(q) = 1$ by definition) allows the scaling of data to an absolute scale, which is important for the accuracy of data analysis. While data modeling was limited by the truncation of reflectivity at $q \sim 0.1$, these data could be qualitatively fitted to estimate the changes in bilayer surface coverage during the reaction and to obtain a qualitative picture of the initial interaction of PLA_2 with different lipids. After several hours of hydrolysis, when either most of the bilayer had been removed or the rate had become very slow, the reflectivity recorded was up to $q = 0.25$ Å^{-1} at two angles, 0.8° and 3°, in a 1.5 h measurement.

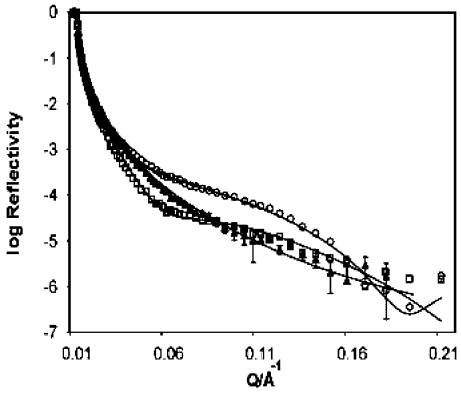

FIGURE 2: DOPC bilayer before and after hydrolysis: (filled triangles) SiO_2 substrate in D_2O; (open circles) DOPC bilayer in D_2O; (open squares) DOPC bilayer 4 h and 10 min after injection of 0.01 mg/mL PLA_2.

The reflectivity profiles of phospholipid−PLA_2 bilayers were analyzed using the phospholipid bilayer structure as a reference. The phospholipids were modeled assuming that, on average, they maintain their planar arrangement during hydrolysis and that the average molecular area remains constant across the layer. Hydrolysis was assumed to lead to desorption of some of the bilayer material, but the presence of products was assumed to leave the bilayer scattering length at a given surface excess unchanged. Hence, the largest contribution to changes in reflectivity arises from the decrease in bilayer surface coverage. As the hydrolysis proceeds, it is possible that gaps and holes are created in the bilayer, as has been previously observed for PLA_2−phospholipid systems by atomic force microscopy (*30*). The structure determination of neutron reflectivity is based on measuring the scattering length density profile normal to the surface, averaged over the entire illuminated area (typically 65×30 mm^2). The specular reflectivity contains no information about the lateral distribution of molecules over this area, and hence, the average area available per phospholipid molecule determined does not necessarily correspond to the actual volume occupied by individual molecules.

We modeled the PLA_2 interaction by assuming that in order to catalyze hydrolysis of the supported phospholipids the enzyme must reside at the bilayer−water interface or possibly partly submerged into the bilayer. As there is a large contrast between the phospholipids and D_2O, we found the reflectivity to be very sensitive to the overall thickness of the phospholipid−PLA_2 bilayer, despite only small amounts of the enzyme at the interface. The reflectivity of the mixed bilayers could be fitted well with a structure where the enzyme partially penetrates into the upper leaflet and displaces an equivalent volume of phospholipid. No evidence was found for the enzyme penetrating into the lower phospholipid leaflet.

Figure 2 shows the reflectivity profiles of a DOPC bilayer before and after 4 h and 10 min of hydrolysis by 0.01 g/L

Table 3: DOPC Bilayer before and after *Naja mossambica mossambica* PLA_2 Hydrolysis

lipid	layer	ρ^a ($\times 10^{-6}$ Å^{-2})	$\rho_\alpha{}^b$ ($\times 10^{-6}$ Å^{-2})	d (Å)	ϕ	A_a (Å^2)	Γ (mg m^{-2})
DOPC	head	1.78	3.47 ± 0.2	6 ± 1	0.63 ± 0.05	89 ± 26	2.9 ± 0.5
Tris pH 7.4	chains	−0.21	1.36 ± 0.1	29 ± 2	0.76 ± 0.02	89 ± 9	2.9 ± 0.5
cobra PLA_2	head 1	1.78	4.25 ± 0.2	5 ± 1	0.46 ± 0.05	144 ± 53	1.8 ± 0.4 (−38%)
0.01 g/L	chains	−0.21	2.94 ± 0.1	26 ± 2	0.52 ± 0.02	143 ± 18	1.8 ± 0.4 (−38%)
4 h 10 min[c]	head 2 + PLA_2	2.35	4.51 ± 0.2	5 ± 1	0.46 ± 0.05	144 ± 53	1.8 ± 0.4 (−38%)
	PLA_2[d]	3.61	5.53 ± 0.2	21 ± 3	0.30 ± 0.07	3700 ± 1700	1.2 ± 1.1

[a] ρ = molecular scattering length density. [b] ρ_a = total scattering length density of layer a. Head 1 refers to the headgroup layer facing the silicon surface. [c] Reflectivity was fitted assuming that the enzyme penetrates 5 Å into the outer headgroup region of the bilayer. [d] Molecular parameters are calculated for the total thickness of the layer containing PLA_2, using the molecular volume and volume fraction of PLA_2.

Table 4: POPC Bilayer before and after *Naja mossambica mossambica* PLA_2 Hydrolysis

lipid	layer	ρ^a ($\times 10^{-6}$ Å^{-2})	$\rho_\alpha{}^b$ ($\times 10^{-6}$ Å^{-2})	d (Å)	ϕ	A_a (Å^2)	Γ (mg m^{-2})
POPC	head	1.86	4.11 ± 0.2	6 ± 1	0.50 ± 0.05	107 ± 33	2.35 ± 0.4
pH 7.35	chains	−0.28	2.37 ± 0.1	29 ± 2	0.60 ± 0.02	107 ± 12	2.35 ± 0.4
cobra PLA_2	head 1	1.86	2.73 ± 0.2	3 ± 1	0.4 ± 0.05	161 ± 62	1.56 ± 0.3 (−34%)
0.01 g/L	chains	−0.28	2.84 ± 0.1	15 ± 2	0.55 ± 0.02	162 ± 24	1.56 ± 0.3 (−34%)
6 h[c]	chains + PLA_2	1.08	3.56 ± 0.1	5 ± 1	0.55 ± 0.02	162 ± 24	1.56 ± 0.3 (−34%)
	head 2 + PLA_2	2.47	4.95 ± 0.2	5 ± 1	0.4 ± 0.05	161 ± 62	1.56 ± 0.3 (−34%)
	PLA_2[d]	3.61	5.38 ± 0.19	22 ± 2	0.35 ± 0.07	2010 ± 705	2.19 ± 2.1

[a] ρ = molecular scattering length density. [b] ρ_a = total scattering length density of layer a. Head 1 refers to the headgroup layer facing the silicon surface. [c] Reflectivity was fitted assuming that the enzyme penetrates 5 Å into the outer headgroup region of the bilayer. [d] Molecular parameters are calculated for the total thickness of the layer containing PLA_2, using the molecular volume and volume fraction of PLA_2.

PLA_2. The silica substrate reflectivity is shown in comparison. It is immediately obvious from the lowered contrast that a significant amount (38%, as given in Table 3) of the bilayer material has been removed from the interface.

The molecular parameters for both phospholipids and enzyme (and the related errors) were derived directly from the fitting variables, namely the thickness of each layer (e.g. headgroups) and the volume fraction of solvent in each layer. Using the molecular volumes and component volumes listed in Table 1, the actual volume occupied by each molecule or molecular fragment (e.g. headgroups) is calculated, and using the layer thickness, the molecular area and, hence, the surface excess are obtained. The results from fitting the reflectivity from the DOPC−PLA_2 bilayer 4 h and 10 min after enzyme injection are shown in Table 3 with a comparison to the original DOPC bilayer. The results indicate that 62% of the bilayer mass remains on the surface along with a diffuse 20 Å thick layer of the enzyme. Although a reasonable fit to the data could be obtained with no penetration of the enzyme into the bilayer, the fit was improved if the enzyme molecules are partially embedded in the headgroup region of DOPC. This is determined by constraining the phospholipid molecular area to be the same on both sides of the bilayer, which requires that an increased scattering length density of 2.15 $\times 10^{-6}$ Å^{-2} is assigned to the outer headgroups in order to provide a fit to the observed reflectivity. We interpret this value to be a consequence of a mixture of 80% DOPC and 20% PLA_2, calculated as indicated in eq 2.

There are two types of fitting error quoted in the tables of results. The errors in thickness, scattering length density, and volume fraction for any single sublayer are estimated from the maximum variation in the acceptable fit subject to the constraints of space-filling and stoichiometry. However, because variations in sublayer structure are highly coupled in scattering length density, the overall errors in surface coverage and bilayer thickness are reduced to ±10% and ±2 Å, respectively. A roughness of 1−3 Å at a given interface would have more or less the same effect on the reflectivity as a ±1−3 Å uncertainty in the thickness of the layers, but it was not necessary to include roughness in the bilayer models in order to improve that fit to the data.

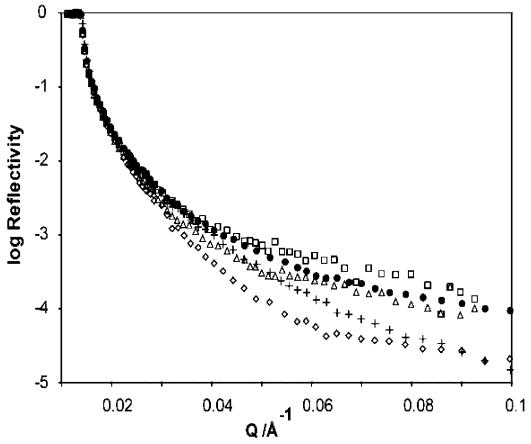

FIGURE 3: Reflectivity changes during the initial stages of *Naja mossambica mossambica* PLA_2 hydrolysis of DOPC recorded at $\theta = 0.8°$ (0.01 Å$^{-1} > q > 0.1$ Å^{-1}) at 10−20 min intervals: (crosses) Si−SiO_2 substrate in D_2O; (filled circles) DOPC bilayer in 10 mM D_2O-Tris buffer at pH 7.35; (open squares) DOPC bilayer 10 min after PLA_2 injection; (open triangles) DOPC 80 min after PLA_2 injection; (open diamonds) DOPC bilayer 4 h and 10 min after PLA_2 injection.

A model illustrating our interpretation of the mean enzyme location and the DOPC bilayer structure used in data fitting is shown in Figure 4b. The bilayer water content is taken to be a composite of the natural headgroup hydration and water occupying the bilayer defects.

Figure 3 shows a set of reflectivity profiles recorded at 10−20 min intervals at $\theta = 0.8°$ during the initial stages of DOPC hydrolysis. There is a small increase in reflectivity during the first 10 min after PLA_2 injection, indicating association of the enzyme with the bilayer. As observed by ellipsometry, the *Naja m. mossambica* PLA_2 begins to hydrolyze DOPC immediately, and the reflectivity results

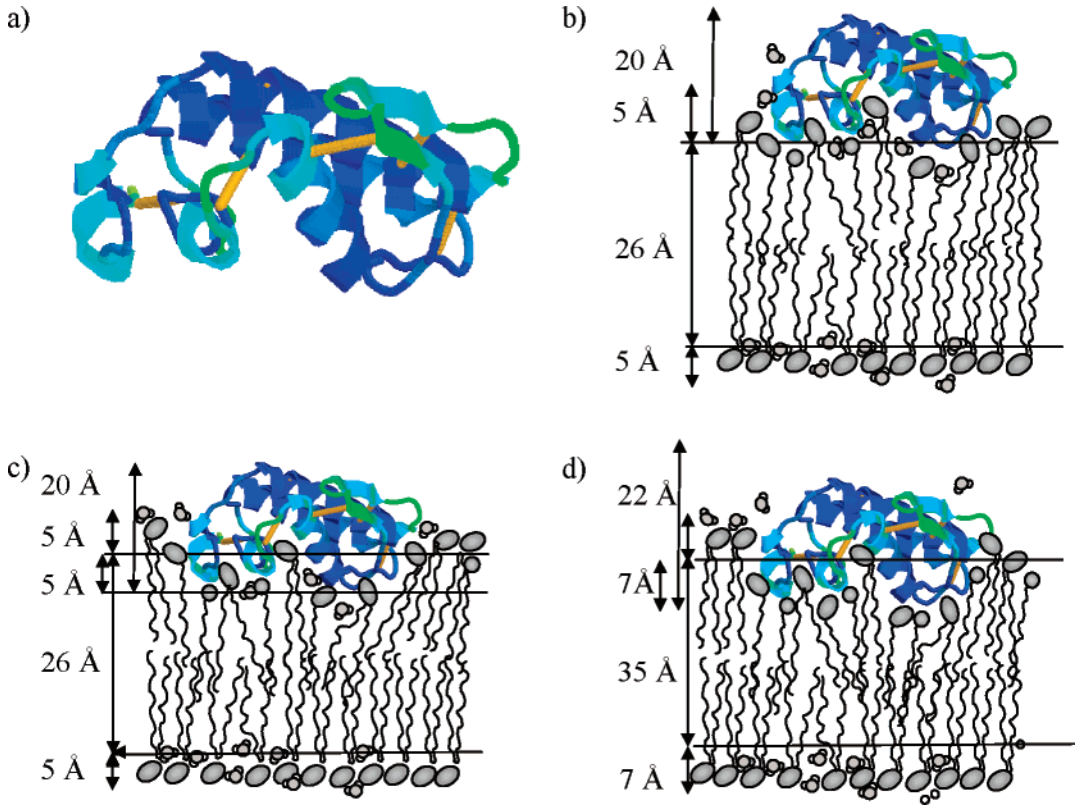

FIGURE 4: (a) Ribbon structure of PLA_2 from *Naja naja naja* venom (pdb IA3D) (*44*). (b) A model for the interaction of PLA_2 with DOPC. The enzyme is located in a 20 Å thick layer at the membrane−water interface and penetrates into the outer headgroup region of the bilayer and 5 Å. (c) A model for the interaction of PLA_2 with POPC, with enzyme penetration through the outer headgroup region by 5 Å into the outer chain region. (d) A model for the interaction of PLA_2 with POPC, with enzyme penetration through the outer headgroup region and 5 Å into the outer chain region.

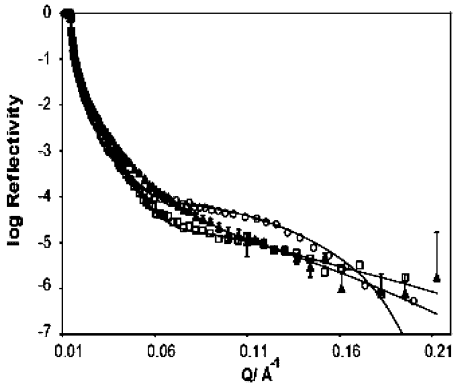

FIGURE 5: POPC bilayer before and after hydrolysis: (filled triangles) SiO_2 substrate in D_2O; (open circles) POPC bilayer in D_2O; (open squares) POPC bilayer 6 h after injection of 0.01 mg/mL PLA_2.

show that, after 80 min, the reflectivity has started to decrease, indicating a decreasing surface excess.

The reflectivity profiles of a POPC bilayer before and after hydrolysis are presented in Figure 5, and the results derived from data fits are summarized in Table 3. In comparison with the case of DOPC, only 34% of the original bilayer material is removed during 6 h of hydrolysis, representing the same trend as seen in the ellipsometry data, that is, that although the rates for DOPC and POPC were very similar, the surface excess of the amount of POPC remaining on the surface was higher than that for DOPC.

The results in Table 4 are illustrated in Figure 4c, showing a model of the POPC−PLA_2 bilayer. In contrast to DOPC, PLA_2 penetrates 5 ± 1 Å into the chain region as well as the headgroups of the outer POPC leaflet. Also, the scattering length densities fitted to this region and the outer headgroups correspond to 35% of the lipid volume being replaced by the enzyme, which is 5% higher than that in the DOPC bilayer.

The presence of 5% more PLA_2 in the POPC bilayer is also supported by the kinetic data (not shown) recorded at the same time intervals as those for the initial hydrolysis of DOPC. The initial increase in reflectivity is larger for POPC, and both of these findings are consistent with the ellipsometry observation that the initial rate of POPC hydrolysis was twice that of DOPC. DOPC and POPC form fluid supported bilayers, which are of similar density. This difference in the volume fraction of PLA_2 at the interface and the rate information support the idea of enzyme penetration into the membranes, because they are a clear demonstration that a small difference in the lipid chains has a regulating effect on the enzyme.

The chain melting temperature of DPPC is 41 °C, and it forms condensed bilayers at room temperature. By ellipsometry it was found that PLA_2 hydrolysis appears to stop after only 14% of the bilayer material has left the interface, and the neutron reflection results confirm this observation, as only 11% of the bilayer is removed by PLA_2. The reflectivity of a DPPC bilayer before and after 6 h and 40 min of cobra PLA_2 hydrolysis is shown in Figure 6. The results are summarized in Table 5, and again, the enzyme is found to penetrate 5 Å into the outer chain region, replacing

Table 5: Properties of an L-α-DPPC Bilayer before and after *Naja Mossambica Mossambica* PLA_2 Hydrolysis

lipid	layer	ρ^a ($\times 10^{-6}$ Å^{-2})	$\rho_\alpha{}^b$ ($\times 10^{-6}$ Å^{-2})	d (Å)	ϕ	A_a (Å^2)	Γ (mg m^{-2})
L-DPPC	head	1.84	3.69 ± 0.2	8 ± 1	0.59 ± 0.05	69 ± 16	3.51 ± 0.5
pH 7.35	chains	−0.36	1.85 ± 0.1	38 ± 2	0.67 ± 0.02	70 ± 6	3.51 ± 0.5
cobra PLA_2	head 1	1.84	3.64 ± 0.2	7 ± 1	0.6 ± 0.05	77 ± 20	3.13 ± 0.5 (−15%)
0.01 g/L	chains	−0.36	1.99 ± 0.1	30 ± 2	0.65 ± 0.02	78 ± 7	3.13 ± 0.5 (−15%)
6 h 40 min	chains + PLA_2	0.44	2.51 ± 0.1	5 ± 1	0.65 ± 0.02	78 ± 7	3.13 ± 0.5 (−15%)
	head 2 + PLA2	2.19	3.85 ± 0.2	7 ± 1	0.6 ± 0.05	77 ± 20	3.13 ± 0.5 (−15%)
	PLA_2	3.61	5.80 ± 0.2	22 ± 2	0.20 ± 0.07	3510 ± 1600	1.25 ± 1.2

[a] ρ = molecular scattering length density. [b] ρ_a = total scattering length density of layer a. Head 1 refers to the headgroup layer facing the silicon surface. [c] Reflectivity was fitted assuming that the enzyme penetrates 5 Å into the outer headgroup region of the bilayer. [d] Molecular parameters are calculated for the total thickness of the layer containing PLA_2, using the molecular volume and volume fraction of PLA_2.

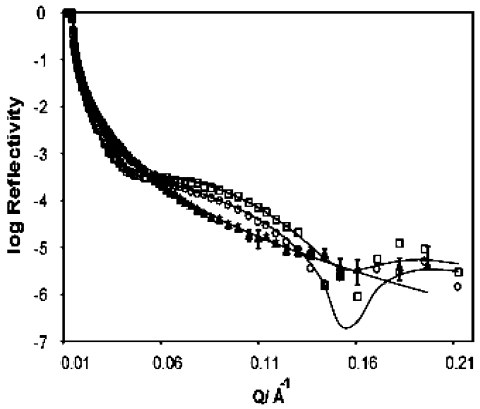

FIGURE 6: DPPC bilayer before and after hydrolysis: (filled triangles) SiO_2 substrate in D_2O; (open circles) DPPC bilayer in D_2O; (open squares) DPPC bilayer 6 h after injection of 0.01 mg/mL PLA_2.

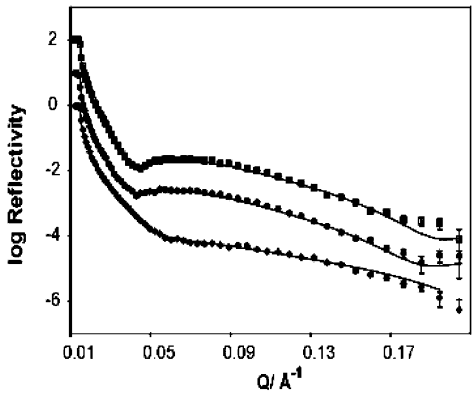

FIGURE 7: Porcine pancreatic PLA_2 adsorption on a hydrophobic surface: (open diamonds) self-assembled d_{27}-octadecyl trichlorosilane monolayer on Si−SiO_2 in D_2O; (open circles) 0.02 mg/mL porcine pancreatic PLA_2 in 10 mM Tris-HCl (D_2O); (open squares) porcine pancreatic PLA_2 after D_2O rinse. Experimental error bars are indicated on each reflectivity profile. The solid lines indicate data fits to the reflectivity using the parameters listed in Table 7.

20% of the lipid volume. A model representation of the structure is given in Figure 4d.

The increase in reflectivity during the first 10 min after PLA_2 injection is much smaller for DPPC than for DOPC or POPC, suggesting that the initial binding of the enzyme to the condensed bilayer is weaker. Both reaction products from DPPC have saturated chains and are less likely to partition out of the bilayer. One possible reason for the short reaction with PLA_2 is that all the fatty acid produced condenses the bilayer to such an extent that the enzyme can no longer access the bonds to be hydrolyzed. If the enzyme penetrates into the bilayer, it may simply become trapped into fatty-acid-rich regions, as has been observed in monolayers.

The results obtained on phospholipid hydrolysis at the silicon−D_2O interface demonstrate that neutron reflectivity can be used to monitor changes in bilayer structure and composition during a surface reaction, and support the idea of phospholipase A_2 penetration into the bilayer.

Given the uncertainty in the reasons for the different PLA_2 interactions with different neutral lipid systems, we investigated the adsorption of porcine pancreatic phospholipase A_2 on a hydrophobic self-assembled monolayer. Although this enzyme belongs to a different class, its catalytic site and tertiary structure are very similar to those of the *Naja mossambica mossambica* PLA_2. The reflectivity results on a deuterated octadecyltrichlorosilane (*d*-OTS) in D_2O in Figure 7 show strong and irreversible adsorption of a dense enzyme layer. The fitted results are summarized in Table 6.

Upon introduction of 0.01 g/L porcine pancreatic PLA_2, a 21 Å layer with a volume fraction of 80% PLA_2 is adsorbed, and no more is adsorbed from a 0.02 g/L solution, nor is any removed upon rinsing with D_2O. After being left overnight at 25 °C, the enzyme remains in a 22 Å layer with a surface excess of 5.3 mg m^{-2}. The area per enzyme molecule is 875 Å^2, and each enzyme is associated with 64 water molecules. These dimensions correlate well with the molecular dimensions, and it is therefore probable that the enzyme retains its tertiary structure, which is very robust and supported by seven disulfide bridges. Adsorption at hydrophobic surfaces has been studied for a number of soluble proteins, for example, lysozyme (*57*), β-casein (*58*), and β-lactoglobulin (*59*), and in most cases the adsorption is irreversible, while denaturation depends on the details of the protein−surface interactions.

The strong and irreversible adsorption of PLA_2 on a hydrophobic, uncharged surface promotes the hypothesis that the enzyme penetrates into the hydrophobic chain region of phospholipid bilayers during hydrolysis and that electrostatic interactions between PLA_2 and the interface act to stabilize the enzyme in a position that allows it to hydrolyze the ester bonds.

5. DISCUSSION

The pattern of hydrolysis of the three different lipids DOPC, POPC, and DPPC by cobra venom phospholipase A_2 is very similar in both neutron reflection and ellipsometry. The rate of hydrolysis and extent of reaction decrease with increasing lipid saturation, and this can be attributed to the increasing hydrophobicity of the reaction product mixture. Neutron reflection additionally shows that the penetration

Table 6: Interaction of Porcine Pancreatic PLA_2 with a Deuterated Octadecyl Trichlorosilane (*d*-OTS) Monolayer at 25 °C

lipid	layer	ρ^a ($\times 10^{-6}$ Å^{-2})	$\rho_\alpha{}^b$ ($\times 10^{-6}$ Å^{-2})	d (Å)	ϕ	A_a (Å^2)	Γ (mg m^{-2})
block Z *d*-OTS	*d*-OTS	6.41	6.40 ± 0.01	32 ± 2	0.80 ± 0.10	21 ± 5	6.67 ± 1.9
	air/vapor	0.00	1.21 ± 0.32	6 ± 1	0.81 ± 0.05		
0.01 g/L	*d*-OTS	6.41	6.40 ± 0.01	33 ± 2	0.80 ± 0.10	21 ± 4	6.88 ± 1.9
pancreatic PLA_2	PLA_2	3.33	3.33 ± 0.21	21 ± 3	1.00 ± 0.07	733 ± 187	6.33 ± 2.2
D_2O rinse	*d*-OTS	6.31	6.32 ± 0.004	31 ± 2	0.80 ± 0.10	22 ± 5	6.47 ± 1.8
	PLA_2	3.84	4.34 ± 0.18	22 ± 3	0.8 ± 0.07	875 ± 235	5.31 ± 2.0

[a] ρ = molecular scattering length density. [b] ρ_a = total scattering length density of layer a. Head 1 refers to the headgroup layer facing the silicon surface. [c] Reflectivity was fitted assuming that the enzyme penetrates 5 Å into the outer headgroup region of the bilayer. [d] Molecular parameters are calculated for the total thickness of the layer containing PLA_2, using the molecular volume and volume fraction of PLA_2.

depth of this enzyme is smallest for DOPC and increases for POPC and DPPC to extend to the lipid chain region. The amount of bound enzyme, however, showed a weak maximum for POPC (30% of lipid volume). The amounts of enzyme in DOPC and DPPC bilayers were comparable, even though the enzyme hydrolyses DOPC much faster than DPPC. However, a significant amount of surfactant was found to be present in the final DOPC bilayers, and its role cannot be ignored. Although 28% of surfactant should act as a diluting agent on DOPC surface concentration, it appears to lead to an increased reaction rate, which suggests that either it disturbs the lipid packing so that the ester bonds are more easily accessible to PLA_2 or its presence increases the strength of enzyme binding to the mixed layer compared to a pure DOPC bilayer. No literature reference was found on pure DOPC substrates to compare with the rates seen on the mixed layers. Otherwise, the increased penetration depth of the enzyme into DPPC seems to serve as an inhibiting effect, which would be consistent with significant accumulation and phase separation of palmitic acid, which is known to increase the packing density of DPPC (*54*). Accompanying the formation of what are thought to be product-rich domains in DPPC and other monolayers containing palmitic acid, phase separation of the enzyme itself into condensed domains has been observed by fluorescence microscopy (*24*, *25*).

Finally, the interaction of PLA_2 with a hydrophobic self-assembled monolayer was found to be irreversible and produced an adsorbed layer whose dimensions correlate well with the molecular dimensions of the enzyme, suggesting that it retains its conformation. PLA_2's have one of the most robust tertiary structures held together by seven disulfide bridges (*16*), so this is not surprising. The strength of the interaction with an uncharged monolayer also suggests that a hydrophobic force plays a major role in the enzyme binding and activity at lipid interfaces.

6. CONCLUSION

To conclude, neutron reflection experiments on phospholipase A_2 strongly support the idea that the enzyme does indeed penetrate into membranes during hydrolysis and that supported phosphatidylcholine bilayers become unstable to compositional changes caused by hydrolysis. The combination of these two observations suggests a means by which PLA_2 hydrolysis can be regulated by lipid chain interactions.

The chemical difference between the three lipids lies mainly in the hydrophobicity and packing order of the lipid chains and in the properties of the product mixture. Palmitic acid is only produced in the hydrolysis of DPPC, and the striking difference in the extent of reaction compared to DOPC and POPC suggests that it plays a major role. Saturated fatty acids are known to make condensed phospholipid bilayers more rigid, whereas unsaturated fatty acids have a negligible effect. Also, aggregation of DPPC reaction products and phase separation of the enzyme have been directly observed by fluorescence microscopy, which is consistent with the idea that, as the enzyme becomes more and more strongly bound to the fatty-acid-rich membrane, it eventually becomes trapped and can no longer release the products or access the next substrate molecule. This would mean that PLA_2 regulation would mainly be a nonspecific interfacial control on the enzyme activity rather than a mechanism inhibiting/promoting the chemical catalytic step itself.

LIST OF SYMBOLS

b = coherent neutron scattering length
ρ = scattering length density of a molecule or fragment
ρ_a = scattering length density of layer a including solvent
q = momentum transfer = $(4\pi \sin \theta)/\lambda$
λ = wavelength
r = Fresnel reflection coefficient
t = Fresnel transmission coefficient
R = intensity of reflection
θ = grazing angle of reflection
N = optical refractive index = $n - jk$
β = phase thickness = $(2\pi/\lambda)nd \sin \theta$
n = neutron refractive index
d = layer thickness
ψ = ratio of reflected p and s polarized light; $\tan \psi = r_p/r_s$
Δ = phase difference between reflected p and s polarized light
A = area per molecule
ϕ_i = volume fraction of component i
Γ = surface excess
V_m = molecular volume

REFERENCES

1. Gelb, M. H., Min, J. H., and Jain, M. K. (2000) Do membrane-bound enzymes access their substrates from the membrane or aqueous phase: interfacial versus noninterfacial enzymes, *Biochim. Biophys. Acta—Mol. Cell Biol. Lipids 1488*, 20−27.
2. Six, D. A., and Dennis, E. A. (2000) The expanding superfamily of phospholipase A(2) enzymes: classification and characterization, *Biochim. Biophys. Acta—Mol. Cell Biol. Lipids 1488*, 1−19.
3. Dijkstra, B. W., Drenth, J., and Kalk, K. H. (1981) Active-Site and Catalytic Mechanism of Phospholipase-A2, *Nature 289*, 604−606.
4. Winstead, M. V., Balsinde, J., and Dennis, E. A. (2000) Calcium-independent phospholipase A(2): structure and function, *Biochim. Biophys. Acta—Mol. Cell Biol. Lipids 1488*, 28−39.
5. Nigam, S., and Schewe, T. (2000) Phospholipase A(2)S and lipid peroxidation, *Biochim. Biophys. Acta—Mol. Cell Biol. Lipids 1488*, 167−181.
6. Sugar, I. P., Mizuno, N. K., Momsen, M. M., Momsen, W. E., and Brockman, H. L. (2003) Regulation of lipases by lipid−lipid interactions: implications for lipid-mediated signaling in cells, *Chem. Phys. Lipids 122*, 53−64.

7. Murakami, M., Nakatani, Y., Kuwata, H., and Kudo, I. (2000) Cellular components that functionally interact with signaling phospholipase A(2)S, *Biochim. Biophys. Acta—Mol. Cell Biol. Lipids 1488*, 159−166.
8. Dessen, A. (2000) Structure and mechanism of human cytosolic phospholipase A(2), *Biochim. Biophys. Acta—Mol. Cell Biol. Lipids 1488*, 40−47.
9. Gijon, M. A., Spencer, D. M., and Leslie, C. C. (2000) in *Advances in Enzyme Regulation*, Vol. 40, pp 255−268, Elsevier Science BV, Amsterdam.
10. Cho, W. (2000) Structure, function, and regulation of Group V phospholipase A(2), *Biochim. Biophys. Acta—Mol. Cell Biol. Lipids 1488*, 48−58.
11. Leslie, C. C. (2004) Regulation of the specific release of arachidonic acid by cytosolic phospholipase A(2), *Prostaglandins, Leukotrienes Essent. Fatty Acids 70*, 373−376.
12. Leslie, C. C. (2004) Regulation of arachidonic acid availability for eicosanoid production, *Biochem. Cell Biol.—Biochim. Biol. Cell. 82*, 1−17.
13. Nevalainen, T. J., Haapamaki, M. M., and Gronroos, J. M. (2000) Roles of secretory phospholipases A(2) in inflammatory diseases and trauma, *Biochim. Biophys. Acta—Mol. Cell Biol. Lipids 1488*, 83−90.
14. Yedgar, S., Lichtenberg, D., and Schnitzer, E. (2000) Inhibition of phospholipase A(2) as a therapeutic target, *Biochim. Biophys. Acta—Mol. Cell Biol. Lipids 1488*, 182−187.
15. Jorgensen, K., Davidsen, J., and Mouritsen, O. G. (2002) Biophysical mechanisms of phospholipase A2 activation and their use in liposome-based drug delivery, *FEBS Lett. 531*, 23−27.
16. Arni, R. K., and Ward, R. J. (1996) Phospholipase A(2)—A structural review, *Toxicon 34*, 827−841.
17. Ward, R. J., De Azevedo, W. F., and Arni, R. K. (1998) At the interface: Crystal structures of phospholipases A(2), *Toxicon 36*, 1623−1633.
18. Scott, D. L., White, S. P., Otwinowski, Z., Yuan, W., Gelb, M. H., and Sigler, P. B. (1990) Interfacial Catalysis—The Mechanism of Phospholipase-A2, *Science 250*, 1541−1546.
19. Pan, Y. H., Epstein, T. M., Jain, M. K., and Bahnson, B. J. (2001) Five coplanar anion binding sites on one face of phospholipase A(2), relationship to interface binding, *Biophys. J. 80*, 255.
20. Hoyrup, P., Jorgensen, K., and Mouritsen, O. G. (2002) Phospholipase A(2)—An enzyme that is sensitive to the physics of its substrate, *Europhys. Lett. 57*, 464−470.
21. Hoyrup, P., Mouritsen, O. G., and Jorgensen, K. (2001) Phospholipase A(2) activity towards vesicles of DPPC and DMPC−DSPC containing small amounts of SMPC, *Biochim. Biophys. Acta—Biomembranes 1515*, 133−143.
22. Honger, T., Jorgensen, K., Stokes, D., Biltonen, R. L., and Mouritsen, O. G. (1997) Lipases, Part B, in *Methods in Enzymology*, Vol. 286, pp 168−190, Academic Press, San Diego.
23. Berg, O. G., and Jain, M. K. (2002) *Interfacial Enzyme Kinetics*, John Wiley & Sons, Ltd., Chichester.
24. Panaiotov, I., and Verger, R. (2000) in *Physical Chemistry of Biological Interfaces* (Baszkin, A., and Norde, W., Eds.) pp 359−400, Marcel Dekker Inc., New York.
25. Maloney, K. M., Grandbois, M., Grainger, D. W., Salesse, C., Lewis, K. A., and Roberts, M. F. (1995) Phospholipase a(2) Domain Formation in Hydrolyzed Asymmetric Phospholipid Monolayers at the Air/Water Interface, *Biochim. Biophys. Acta—Biomembranes 1235*, 395−405.
26. Burns, A. R. (2003) Domain structure in model membrane bilayers investigated by simultaneous atomic force microscopy and fluorescence imaging, *Langmuir 19*, 8358−8363.
27. Li, J. B., Chen, Z. J., Wang, X. L., Brezesinski, G., and Mohwald, H. (2000) Dynamic observations of the hydrolysis of a DPPC monolayer at the air/water interface catalyzed by phospholipase A(2), *Angew. Chem., Int. Ed. 39*, 3059−3062.
28. Yu, B. Z., Ghomashchi, F., Cajal, Y., Annand, R. R., Berg, O. G., Gelb, M. H., and Jain, M. K. (1997) Use of an imperfect neutral diluent and outer vesicle layer scooting mode hydrolysis to analyze the interfacial kinetics, inhibition, and substrate preferences of bee venom phospholipase A(2), *Biochemistry 36*, 3870−3881.
29. Balashev, K., Jensen, T. R., Kjaer, K., and Bjornholm, T. (2001) Novel methods for studying lipids and lipases and their mutual interaction at interfaces. Part I. Atomic force microscopy, *Biochimie 83*, 387−397.
30. Nielsen, L. K., Risbo, J., Callisen, T. H., and Bjornholm, T. (1999) Lag-burst kinetics in phospholipase A(2) hydrolysis of DPPC bilayers visualized by atomic force microscopy, *Biochim. Biophys. Acta—Biomembranes 1420*, 266−271.
31. Callisen, T. H., and Talmon, Y. (1998) Direct imaging by cryo-TEM shows membrane break-up by phospholipase A(2) enzymatic activity, *Biochemistry 37*, 10987−10993.
32. Tiberg, F., Harwigsson, I., and Malmsten, M. (2000) Formation of model lipid bilayers at the silica-water interface by coadsorption with nonionic dodecyl maltoside surfactant, *Eur. Biophys. J. Biophys. Lett. 29*, 196−203.
33. Vacklin, H., Tiberg, F., Fragneto G., Thomas R. K. (2004) Formation of supported phospholipid bilayers via coadsorption with β-D-dodecyl maltoside, *Biophys. Biochim. Acta—Biomembranes* (in press).
34. Vacklin, H., Tiberg, F., Fragneto, G., Thomas, R. K. (2004) Composition of supported model membranes determined by neutron reflection, *Langmuir* (accepted).
35. Fragneto, G., Li, Z. X., Thomas, R. K., Rennie, A. R., and Penfold, J. (1996) A neutron reflectivity study of the adsorption of aerosol-OT on self-assembled monolayers on silicon, *J. Colloid Interface Sci. 178*, 531−537.
36. Thirtle, P. N. 1997, AFit simulation program, Oxford University (http://physchem.ox.ac.uk/∼rkt/links/software).
37. Crowley, T. L., Lee, E. M., Simister, E. A., and Thomas, R. K. (1991) The Use of Contrast Variation in the Specular Reflection of Neutrons from Interfaces, *Physica B 173*, 143−156.
38. Petrache, H. I., Feller, S. E., and Nagle, J. F. (1997) Determination of component volumes of lipid bilayers from simulations, *Biophys. J. 72*, 2237−2242.
39. Wiener, M. C., and White, S. H. (1992) Structure of a Fluid Dioleoylphosphatidylcholine Bilayer Determined by Joint Refinement of X-ray and Neutron-Diffraction Data III. Complete Structure, *Biophys. J. 61*, 434−447.
40. Small, D. M. (1986) *The Physics and Chemistry of Lipids*, Plenum Press, New York.
41. Costigan, S. C., Booth, P. J., and Templer, R. H. (2000) Estimations of lipid bilayer geometry in fluid lamellar phases, *Biochim. Biophys. Acta—Biomembranes 1468*, 41−54.
42. Nagle, J. F., and Wiener, M. C. (1988) Structure of Fully Hydrated Bilayer Dispersions, *Biochim. Biophys. Acta—Biomembranes 942*, 1−10.
43. Joubert, F. J. (1977) *Naja Mossambica Mossambica* venom: Purifications, some properties and the amino acid sequences of three phospholipases A (CM-I, CM-IIand CM-II). *Biochim. Biophys. Acta 493*, 216−227.
44. RSBC. (2003).
45. Zamyatin, A. A. (1972) Protein Volume in Solution, *Prog. Biophys. Mol. Biol. 24*, 107−123.
46. Jacrot, B. (1976) *Rep. Prog. Phys. 39*, 911.
47. Fragneto, G., Graner, F., Charitat, T., Dubos, P., and Bellet-Amalric, E. (2000) Interaction of the third helix of Antennapedia homeodomain with a deposited phospholipid bilayer: A neutron reflectivity structural study, *Langmuir 16*, 4581−4588.
48. Johnson, S. J., Bayerl, T. M., McDermott, D. C., Adam, G. W., Rennie, A. R., Thomas, R. K., and Sackmann, E. (1991) Structure of an Adsorbed Dimyristoylphosphatidylcholine Bilayer Measured with Specular Reflection of Neutrons, *Biophys. J. 59*, 289−294.
49. Iler, R. K. (1979) *The Chemistry of Silica*, Wiley-Interscience.
50. Landgren, M., and Jonsson, B. (1993) Determination of the Optical-Properties of Si/Sio2 Surfaces by Means of Ellipsometry, Using Different Ambient Media, *J. Phys. Chem. 97*, 1656−1660.
51. Thirtle, P. N. (1999) Oxford University, DPhil Thesis, p 193.
52. Tiberg, F., and Landgren, M. (1993) Characterization of Thin Nonionic Surfactant Films at the Silica Water Interface by Means of Ellipsometry, *Langmuir 9*, 927−932.
53. Azzam, R. M. A., and Bashara, N. M. (1986) *Ellipsometry and Polarised Light*, North-Holland, Amsterdam.
54. Inoue, T., Yanagihara, S., Misono, Y., and Suzuki, M. (2001) Effect of fatty acids on phase behavior of hydrated dipalmitoylphosphatidylcholine bilayer: saturated versus unsaturated fatty acids, *Chem. Phys. Lipids 109*, 117−133.
55. Davidsen, J., Mouritsen, O. G., and Jorgensen, K. (2002) Synergistic permeability enhancing effect of lysophospholipids and fatty acids on lipid membranes, *Biochim. Biophys. Acta—Biomembranes 1564*, 256−262.
56. Cubitt, R., and Fragneto, G. (2002) D17: the new reflectometer at the ILL, *Appl. Phys. A—Mater. Sci. Process. 74*, S329−S331.
57. Lu, J. R., Su, T. J., Thirtle, P. N., Thomas, R. K., Rennie, A. R., and Cubitt, R. (1998) The denaturation of lysozyme layers

adsorbed at the hydrophobic solid/lquid surface studied by neutron reflection, *J. Colloid Interface Sci. 206*, 212−223.

58. Fragneto, G., Thomas, R. K., Rennie, A. R., and Penfold, J. (1995) Neutron Reflection Study of Bovine Beta-Casein Adsorbed on Ots Self-Assembled Monolayers, *Science 267*, 657−660.

59. Fragneto, G., Su, T. J., Lu, J. R., Thomas, R. K., and Rennie, A. R. (2000) Adsorption of proteins from aqueous solutions on hydrophobic surfaces studied by neutron reflection, *Phys. Chem. Chem. Phys. 2*, 5214−5221.

BI047727A